*Journal of Applied Mechanics and Technical Physics, Vol. 47, No. 4, pp. 505–509, 2006*

# TRANSLATIONAL NONEQUILIBRIUM OF A GAS FLOW INTO VACUUM IN A CONSTANT-SECTION CHANNEL

**S. V. Kulikov**

UDC 533.6.011.72:533.72

*A single-species gas flow into vacuum in a constant-section channel is computed by means of the Direct Simulation Monte Carlo method. It is shown that the longitudinal, transverse, and total kinetic temperatures are significantly different in the head part of the flow, which is a consequence of the arising translational nonequilibrium. The flow is almost self-similar in the entire region of flow expansion (except for distributions of the transverse and total kinetic temperatures in the head part of the gas flow), which allows one to predict flow parameters at times greater than those used in simulations.*

**Key words:** *gas, vacuum, statistical simulation.*

**Introduction.** Obviously, there is no clear physical boundary between matter and vacuum in the case of a gas flow into vacuum, whereas such a boundary is used in solving the present problem at the macroscopic level by hydrodynamic methods. In addition, the distribution of molecules in terms of translational degrees of freedom in the head part of the gas flow may differ from the Maxwellian distribution. The flow in a constant-section channel is numerically examined in the present work with the use of direct statistical Monte Carlo (DSMC) method. It should be noted that this method actually allows obtaining a solution of the Boltzmann equation without solving the latter. Moreover, the DSMC method can be used for simulating steady flows formed when a steady state is reached.

The main challenge of the present work is to check self-similarity and to study the translational nonequilibrium of the head part of the gas flow into vacuum in a constant-section channel.

There are many papers dealing with exhaustion of gases into vacuum, but most of them consider different conditions of gas expansion. Only papers [1–3] should be noted. The flow in a constant-section channel was considered in [1, Sec. 99, Problem 2], but this was done at the macroscopic (hydrodynamic) level. Results of statistical simulation of the collisions of gases are also presented in [2, 3]. Before the collisions of flows, the problem coincides with that considered in the present paper, but this stage of evolution of the gas system is given little attention in [2, 3]. It should be noted that the problem of a gas flow into vacuum in a constant-section channel is similar in many aspects to the problem of unsteady evaporation into vacuum from a flat surface (see, e.g., [4]).

**1. Formulation of the Problem and Simulation Technique.** We consider a one-dimensional flow of a single-species gas without internal degrees of freedom in a one-dimensional space of coordinates (the channel has a large constant cross section, and the influence of the side walls is ignored). The gas is initially located in part $A$ of the channel separated by a partition from vacuum located in part $B$ of the channel. When the partition is instantaneously removed, the gas moves into the latter domain. Simulations are performed in the time interval when the molecules have not yet reached the end of part $B$ of the channel.

The DSMC method described in [5–7] and based on the principle of splitting of molecular motion and intermolecular collisions developed in [8] is used in the present computations.

Institute of Problems of Chemical Physics, Russian Academy of Sciences, Chernogolovka 142432; kuls@icp.ac.ru. Translated from Prikladnaya Mekhanika i Tekhnicheskaya Fizika, Vol. 47, No. 4, pp. 54–59, July–August, 2006. Original article submitted April 7, 2005; revision submitted September 2, 2005.

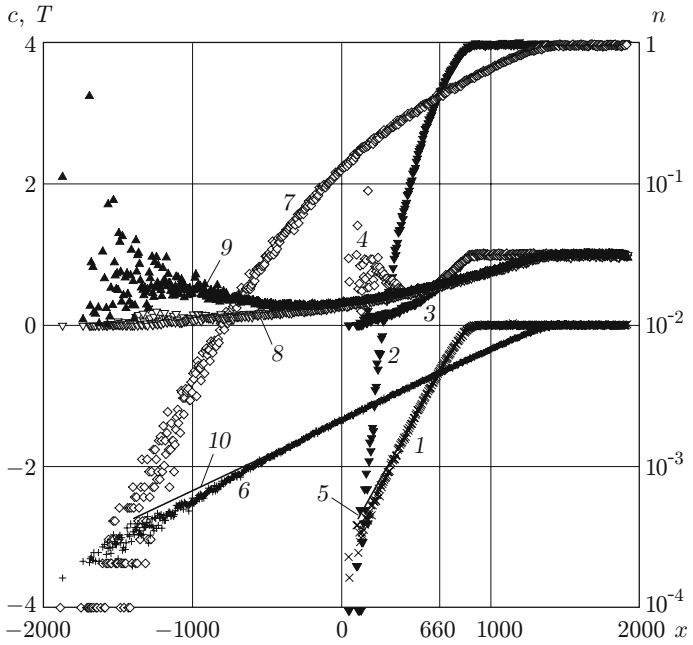


Fig. 1. Profiles of velocity $c$ (1, 5, 6, and 10), concentration $n$ (2 and 7), longitudinal kinetic temperature $T_l$ (3 and 8), and transverse kinetic temperature $T_t$ (4 and 9): curves 1–5 refer to $t = 200\lambda/\nu$ and curves 6–10 refer to $t = 750\lambda/\nu$; curves 5 and 10 show the results of hydrodynamic computations.

The following modeling procedure is used. The simulated medium is replaced by a system of model particles. In accordance with the initial conditions, the particles have certain prescribed initial velocities and are distributed in cells that compose the examined space. Collisions are assumed to be binary and to occur with a certain probability only between particles located in one cell.

The evolution of the considered system during the time interval $\Delta t$ is divided into two stages: 1) pure motion of particles with unchanged velocities during the time $\Delta t$ (stage of displacements); 2) pure change in particle velocities in accordance with the results of sampling with certain probabilities of their collisions during the same time interval with fixed positions of the particles (stage of collisions).

The molecules are considered as hard spheres of identical diameters without any internal structure. The simulations are performed in a one-dimensional space of coordinates and in a three-dimensional space of velocities. In other words, only the streamwise coordinate of particles was considered, whereas all three components of velocity vectors were taken into account in collisions of particle pairs.

The straight-line segment representing the domain of simulation is bounded by walls with elastic reflection of molecules; this segment is divided into 6400 cells of an identical length $\Delta x$. This segment consists of two parts ($A$ and $B$). At the beginning, domain $A$ contains the particles (on the average, 9600 particles in each cell), and the other part is empty. The initial distribution of particle velocity is assumed to be Maxwellian. The time of splitting of the stages of displacements and collisions is $\Delta t = 0.05$ ($\Delta x = 0.6$). Hereinafter, the distance is normalized to the mean free path of molecules in the gas $\lambda$, the velocity is normalized to the most probable thermal velocity of particles $\nu$, and the time is normalized to $\lambda/\nu$. The values of $\lambda$ and $\nu$ are determined at the initial time.

**2. Results and Discussion.** Figure 1 shows the profiles of flow parameters for two times. In this figure, the concentration $n$ and the longitudinal ($T_l$) and transverse ($T_t$) kinetic temperatures are normalized to their initial values in domain $A$. The total kinetic temperature $T_s$ is not plotted to leave the graph readable. Its value can be readily determined from $T_l$ and $T_t$: $T_s = (T_l + 2T_t)/3$. The greater part of the flow corresponds rather accurately to the hydrodynamic self-similar flow in the form of an expansion wave (EW) [1]. These solutions are shown in Fig. 1 as segments of straight lines 5 and 10 for the flow velocity $c$. It should be noted that the real domain of propagation of matter is substantially greater than that obtained in an analytical solution.

TABLE 1

Results of the Solution for $x = 660$

| $t$ | $n$ | $c$ | $T_l$ | $T_t$ | $T_s$ |
|---|---|---|---|---|---|
| 200 | 0.450 | −0.644 | 0.547 | 0.606 | 0.586 |
| 400 | 0.449 | −0.662 | 0.546 | 0.583 | 0.570 |
| 750 | 0.434 | −0.669 | 0.578 | 0.571 | 0.573 |
| Macroscopic theory | 0.422 | −0.685 | — | — | 0.562 |

By virtue of self-similarity, a typical feature of the analytical solution of the form of an expansion wave is constant flow parameters at the point of their initial discontinuity at the boundary between parts $A$ and $B$, which is fairly accurately reproduced in simulations (see Fig. 1 and Table 1, which lists the flow macroparameters at this point with $x = 660$ for different times). It is at this point at the boundary between parts $A$ and $B$ that the above-mentioned specific feature of the flow is observed; no special features are observed at the point $x = 0$. As part $A$ is located on the right, the flow is aligned with the negative direction of the $x$ axis. Flow parameters obtained analytically on the basis of [1] at the same point $x = 660$ are also listed in Table 1. Constant values of macroparameters, which were noted above, confirm the validity of the simulation results.

In the head part of the flow, the values of $T_l$ and $T_t$ are significantly different (see Fig. 1), and $T_t > T_l$. This is a consequence of translational nonequilibrium. In addition, the nonmonotonic shape of the profile $T_t$ should be noted. The leading molecules of the head part of the flow move almost without collisions; therefore, their distribution in terms of transverse velocity should be almost the same as that at the initial time of simulations. For these molecules, we have $T_t = 1$ (see [4]). Though the simulation results for the head part of the flow differ from the analytical solution in the form of an expansion wave [1], they are similar for the time instants considered (see Fig. 1). At least, approximate self-similarity of the flow can be expected. This can be easily verified by overlapping the profiles of flow parameters obtained for different times with changing their scales along the abscissa axis. It turns out that approximate self-similarity is observed at the times $t = 200$, 400, and 750 for all profiles, except for $T_t$ in the head part of the flow. Such a difference arises almost simultaneously with deviation of the simulated velocity profile from the corresponding analytical solution for the EW. The smaller the value of $t$, the greater the value of $T_t$ for identical values of $c$. The distribution of longitudinal temperature is rather self-similar even in the flow region with a large scatter of results. Hence, despite an additional parameter, such as the time of translational relaxation, the simulation results show that the flow has a self-similar character almost in the entire range of flow expansion. This allows one to predict flow parameters at times greater than those used in simulations.

Figure 2 shows the velocity distributions obtained at $t = 750$ at six points corresponding to typical areas of the flow, which illustrate the transition from the state of strong nonequilibrium to equilibrium in terms of translational degrees of freedom. More exactly, the distributions were obtained by sampling the simulation results in the time interval $t = 750.0$–$750.1$. The sampling process was repeated 20 times, each time beginning from the state of the flow at the time $t = 750$ but with a different initial value of the generator of random numbers. In this case, the velocities are normalized to the velocity of sound in the motionless gas $a$ (as is conventionally done), and the distributions themselves are normalized so that their integrals in terms of velocities are equal to unity. The subprogram of velocity distributions was previously used in simulating a steady shock wave. Such normalization is convenient for distributions of longitudinal velocity, because the graph clearly shows the mean velocities ahead of the wave front and behind it, expressed in Mach numbers. Figure 2a shows the distributions of $F_l$ in terms of the longitudinal molecular velocity $c_l$, and Fig. 2b shows the distributions of $F_t$ in terms of the transverse molecular velocity $c_t$ (e.g., projections of velocity onto the $y$ axis). It should be noted that the distribution differs from the Maxwellian form in the head part of the flow (e.g., curve 1 in Fig. 2a) and that the half-width and height of $F_t$ change nonmonotonically (Fig. 2b) in the upstream direction from the head part of the flow. The latter is related to a similar change in the temperature $T_t$. It was noted above that the distribution in terms of transverse velocity should be almost the same as that at the initial time of simulations. Indeed, curves 1 and 6 are close in shape. The number of samplings for distribution 1 is very small, which is responsible for three peaks observed. If the number of samplings were greater, curve 1 would be more smooth and, apparently, the agreement between curves 1 and 6 would be even better. Figure 2c shows the distributions $G$ of the pairs of molecules in terms of the dimensionless

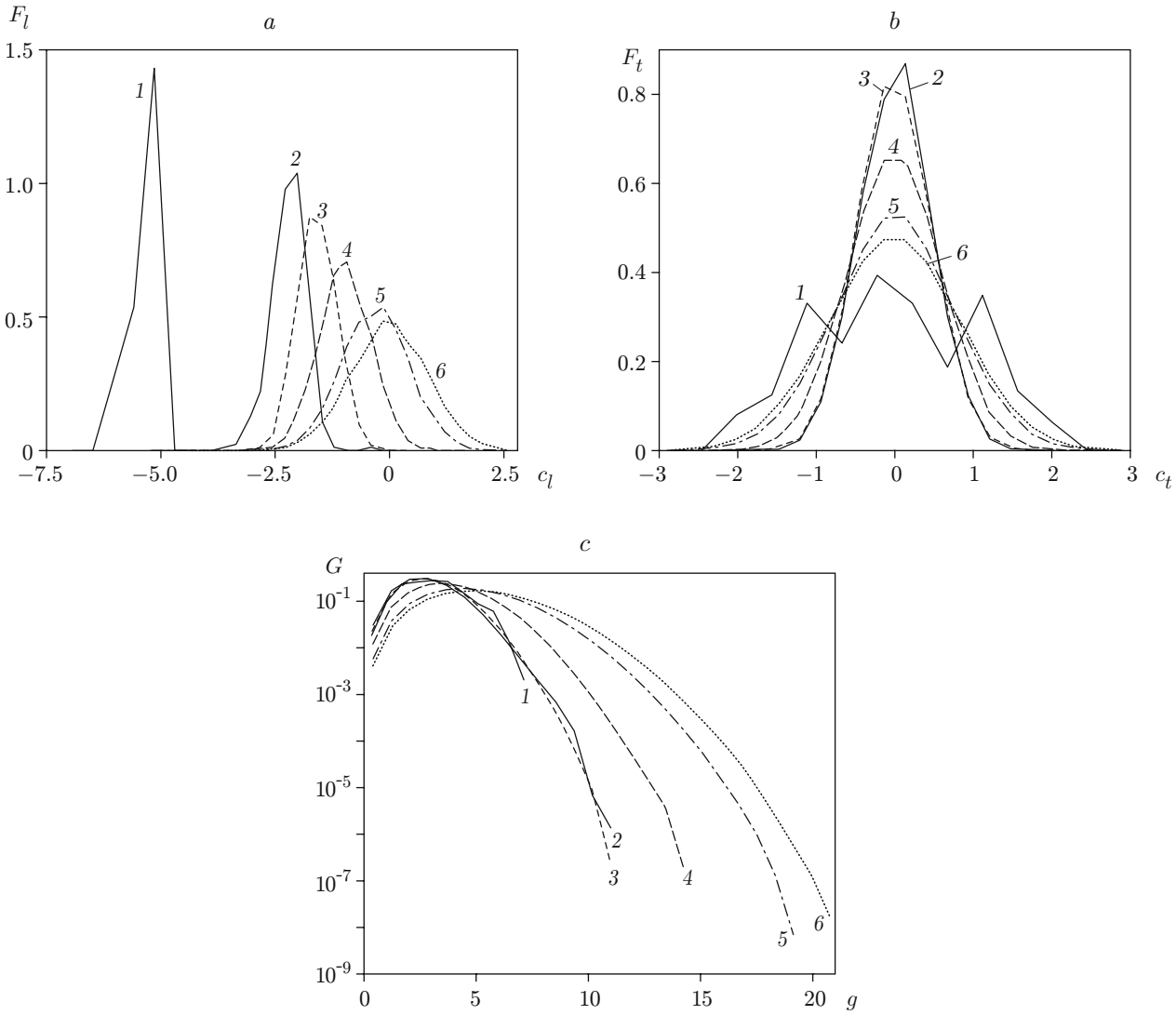


Fig. 2. Distributions of particles in terms of longitudinal (a), transverse (b), and dimensionless (c) velocities at various points of the flow: $x = -1223.7$ (1), $-497.7$ (2), 6.3 (3), 504.3 (4), 1080.3 (5), and 1860.3 (6).

TABLE 2

Root-Mean-Square Errors $\sigma_l$ and $\sigma_g$ of the Distributions of $F_l$ and $G$ at Several Points of the Flow for Several Velocities Normalized to $a$

| $x$ | $c_l$ | $\sigma_l$ | $g$ | $\sigma_g$ |
|---|---|---|---|---|
| −1223.7 | −6.04 | 0.018 | 3.733 | 0.012 |
| | −5.59 | 0.005 | 6.448 | 0.004 |
| | −5.14 | 0.013 | 7.127 | $1.5 \cdot 10^{-3}$ |
| 6.3 | −1.470 | 0.001 | 2.851 | $10^{-4}$ |
| | −0.402 | $3.5 \cdot 10^{-4}$ | 10.181 | $6.8 \cdot 10^{-7}$ |
| | −0.134 | $2 \cdot 10^{-4}$ | 11.000 | $1.4 \cdot 10^{-7}$ |
| 1080.3 | −3.081 | $10^{-4}$ | 0.407 | $1.2 \cdot 10^{-5}$ |
| | −2.817 | $6 \cdot 10^{-5}$ | 3.665 | $4.3 \cdot 10^{-5}$ |
| | 0.671 | $10^{-4}$ | 14.250 | $6.2 \cdot 10^{-8}$ |

velocity $g$. For a pair of molecules, the value of $g$ equals the absolute value of the difference in velocity vectors of these molecules. No specific features are observed in the behavior of $G$. Standard root-mean-square deviations from the mean values (errors) $\sigma_l$ and $\sigma_g$ of the distributions of $F_l$ and $G$ at several points of the flow are given in Table 2 for several values of velocities $c_l$ and $g$. These velocities were chosen to give an idea of the errors at the center and in the "tails" of velocity distributions.

**Conclusions.** In solving the problem, the real range of propagation of matter and the velocity (in absolute value) of the head part of the flow are found to be significantly greater than their values predicted analytically.

The longitudinal, transverse, and total kinetic temperatures in the head part of the flow are substantially different, which results from translational nonequilibrium. The nonmonotonic behavior of the profiles of the transverse and total kinetic temperatures should be noted.

In addition, the simulation results testify to a self-similar character of the flow in the entire range of flow expansion, except for the distributions of transverse and total kinetic temperatures in the head part of the gas flow. This allows one to determine flow parameters at times greater than those used in simulations.

## REFERENCES


1. L. D. Landau and E. M. Lifshits, *Course of Theoretical Physics*, Vol. 6: *Fluid Mechanics*, Pergamon Press, Oxford-Elmsford, New York (1987).
2. A. A. Morozov, M. Yu. Plotnikov, and A. K. Rebrov, "Collision of supersonic flows in vacuum and ambient space," *J. Appl. Mech. Tech. Phys.*, **40**, No. 4, 588–593 (1999).
3. A. A. Morozov, M. Yu. Plotnikov, and A. K. Rebrov, "Comparison of various approaches in simulating collisions of supersonic flows," *Mat. Model.*, **12**, No. 5, 67–73 (2000).
4. G. A. Luk'yanov, "Unsteady exhaustion of vapor into vacuum from a flat surface," *Teplofiz. Aéromekh.*, **11**, No. 1, 63–77 (2004).
5. A. P. Genich, S. V. Kulikov, G. B. Manelis, et al., "The application of weighting schemes in the statistical modelling of flows of multicomponent gas to the calculation of the structure of a shock wave," *Zh. Vychisl. Mat. Mat. Fiz.*, **26**, No. 12, 1839–1854 (1986).
6. A. P. Genich, S. V. Kulikov, G. B. Manelis, and S. L. Chereshnev, "Thermophysics of translational relaxation in shock waves in gases," *Sov. Tech. Rev. B Therm. Phys.*, **4**, Part 1, 1–69 (1992).
7. S. V. Kulikov and M. E. Solov'eva, "Efficiency of statistical simulation of a shock wave in a gas mixture," *Zh. Vychisl. Mat. Mat. Fiz.*, **28**, No. 12, 1867–1873 (1988).
8. G. A. Bird, *Molecular Gas Dynamics*, Clarendon Press, Oxford (1976).